

Sum Rate Maximization for Reconfigurable Intelligent Surface Assisted Device-to-Device Communications

Yashuai Cao, *Student Member, IEEE*, and Tiejun Lv, *Senior Member, IEEE*

Abstract—In this letter, we propose to employ reconfigurable intelligent surfaces (RISs) for enhancing the D2D underlying system performance. We study the joint power control, receive beamforming, and passive beamforming for RIS assisted D2D underlying cellular communication systems, which is formulated as a sum rate maximization problem. To address this issue, we develop a block coordinate descent method where uplink power, receive beamformer and reflection phase shifts are alternatively optimized. Then, we provide the closed-form solutions for both uplink power and receive beamformer. We further propose a quadratic transform based semi-definite relaxation algorithm to optimize the RIS phase shifts, where the original passive beamforming problem is translated into a separable quadratically constrained quadratic problem. Numerical results demonstrate that the proposed RIS assisted design significantly improves the sum-rate performance.

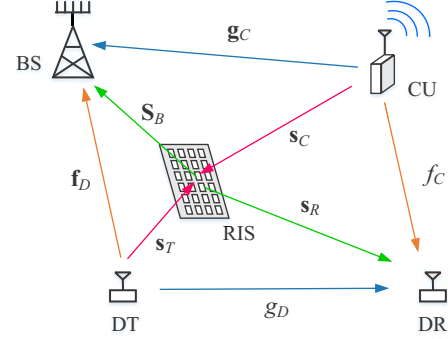


Fig. 1. An RIS assisted D2D underlying cellular system.

I. INTRODUCTION

DEVICE-TO-DEVICE (D2D) communication allows direct communication between users by reusing resources of cellular users (CUs), thus improving network spectral efficiency. Sharing the same spectrum, however, may cause severe interference in D2D underlying cellular communications. To manage the co-channel interference, resource allocation for D2D communications has recently gained an upsurge of interest [1], [2].

Recently, reconfigurable intelligent surface (RIS) has been proposed as a promising technology, which can reconfigure the wireless propagation environment via adjusting the passive beamforming adaptively and properly. As a appealing complementary solution to enhance wireless transmissions, RIS composed of massive low-cost and nearly passive reflective elements can be flexibly deployed in the current networks [3], [4].

RIS is envisioned to achieve the desired power enhancement and interference suppression by passive (reflect) beamforming. In this letter, we introduce RIS into the D2D underlying systems. In our proposed RIS assisted D2D underlying system, inter user interference becomes different from existing works without RIS, which further complicates the resource allocation problem. We aim to maximize the achievable sum-rate of the considered system by jointly designing beamforming and allocating power. To our best knowledge, the impact of RIS reflect gain on the D2D system performance has not been studied yet.

II. SYSTEM MODEL

We study an RIS assisted uplink SIMO system for a D2D underlying cellular network, including an M -antenna base station (BS), an N -element RIS, a single cellular user (CU) and one D2D pair. The D2D users are allowed to reuse the uplink spectrum resource of a CU¹, where these users are equipped with a single antenna. In this work, the BS is responsible for uplink power control of the CU and D2D pair and coordinating their communications. As Fig. 1 shows, $\mathbf{g}_C \in \mathbb{C}^{M \times 1}$ and $g_D \in \mathbb{C}$ are the channels from the CU to the BS and from the D2D transmitter (DT) to the D2D receiver (DR); $f_C \in \mathbb{C}$ and $\mathbf{f}_D \in \mathbb{C}^{M \times 1}$ are the interference channels from the CU to the DR and from the DT to the BS; $\mathbf{s}_C \in \mathbb{C}^{N \times 1}$, $\mathbf{S}_B \in \mathbb{C}^{M \times N}$, $\mathbf{s}_T \in \mathbb{C}^{N \times 1}$ and $\mathbf{s}_R \in \mathbb{C}^{N \times 1}$ are the channels from the CU to the RIS, from the RIS to the BS, from the DT to the RIS and from the RIS to the DR. Let $\Theta = \text{diag}\{e^{j\theta_1}, e^{j\theta_2}, \dots, e^{j\theta_N}\}$ denotes the diagonal phase shift matrix of the RIS. To mitigate the intra-cell interference and strengthen the desired signal, the phase shifts of the RIS and the transmit powers of the CU and the DT should be optimized to maximize the uplink sum rate.

Denoting the transmit power of the DT and the CU by p_D and p_C , the signal-to-interference-plus-noise ratio (SINR) at the DR is given by

$$\gamma_D = \frac{p_D |h_D|^2}{p_C |h_C|^2 + \sigma_D^2}, \quad (1)$$

where $h_D = g_D + \mathbf{s}_R^H \Theta \mathbf{s}_T$, $h_C = f_C + \mathbf{s}_R^H \Theta \mathbf{s}_C$ and σ_D^2 is the noise power at the DR. The uplink received SINR at the BS

¹We assume that CUs are allocated with orthogonal spectrum in a cell, and hence there is no interference among CUs. The intra-cell interference between the D2D pair and the CU is caused when the channel of a CU is reused by D2D devices.

is

$$\gamma_C = \frac{p_C |\mathbf{w}^H \mathbf{h}_C|^2}{p_D |\mathbf{w}^H \mathbf{h}_D|^2 + \sigma_B^2}, \quad (2)$$

where $\mathbf{h}_C = \mathbf{g}_C + \mathbf{S}_B \Theta \mathbf{s}_C$, $\mathbf{h}_D = \mathbf{f}_D + \mathbf{S}_B \Theta \mathbf{s}_T$, $\mathbf{w} \in \mathbb{C}^{M \times 1}$ is the unit-norm receive beamforming vector at the BS, and σ_B^2 is the noise power at the BS.

The uplink sum rate maximization problem subject to transmit power constraints and the SINR requirements can be formulated as

$$\begin{aligned} \text{(P1): } & \max_{\{p_C, p_D, \mathbf{w}, \Theta\}} \log(1 + \gamma_D) + \log(1 + \gamma_C) \\ & \text{s.t. } 0 < p_D \leq p_D^{\max}, \quad (3a) \\ & 0 < p_C \leq p_C^{\max}, \quad (3b) \\ & \gamma_D \geq \gamma_D^{\max}, \quad (3c) \\ & \gamma_C \geq \gamma_C^{\max}, \quad (3d) \\ & \|\mathbf{w}\|^2 = 1, \quad (3e) \\ & \theta_n \in [0, 2\pi), \quad n = 1, 2, \dots, N, \quad (3f) \end{aligned}$$

where p_C^{\max} and p_D^{\max} are the maximum transmit powers of the CU and DT; γ_C^{\max} and γ_D^{\max} are the minimum SINR requirements for the CU and D2D devices, respectively; and (3f) is the phase shift constraints of the RIS.

III. ALTERNATING OPTIMIZATION SCHEME

To make the problem (P1) tractable, we propose to solve it through a block coordinate descent (BCD) approach. The BCD algorithm decouples the optimization variables, thus resulting in three phases, namely receive beamforming, power allocation, and phase-shift design.

A. Receive Beamforming

We start with the uplink receive beamforming when given $\{p_C, p_D\}$ and Θ . Note that the coefficients h_D , h_C , \mathbf{h}_C and \mathbf{h}_D in (1) and (2) are fixed at this point. Therefore, we should find a optimal \mathbf{w} to maximize γ_C . From (2), the receive beamforming problem can be written as

$$\begin{aligned} \text{(P2): } & \max_{\mathbf{w}} \frac{p_C \mathbf{w}^H \mathbf{h}_C \mathbf{h}_C^H \mathbf{w}}{\mathbf{w}^H (p_D \mathbf{h}_D \mathbf{h}_D^H + \sigma_B^2 \mathbf{I}) \mathbf{w}}, \\ & \text{s.t. } (3e), \end{aligned}$$

which is, fortunately, translated into a Rayleigh quotient maximization problem [5]. Due to $p_D \mathbf{h}_D \mathbf{h}_D^H + \sigma_B^2 \mathbf{I} \succ \mathbf{0}$, the optimal \mathbf{w} is given by

$$\hat{\mathbf{w}} = \frac{(p_D \mathbf{h}_D \mathbf{h}_D^H + \sigma_B^2 \mathbf{I})^{-1} \mathbf{h}_C}{\|(p_D \mathbf{h}_D \mathbf{h}_D^H + \sigma_B^2 \mathbf{I})^{-1} \mathbf{h}_C\|}. \quad (5)$$

Plugging (5) into (2) and applying Sherman-Morrison lemma [6], the achievable SINR of the CU can be obtained as

$$\begin{aligned} \max_{\mathbf{w}} \gamma_C &= p_C \mathbf{h}_C (p_D \mathbf{h}_D \mathbf{h}_D^H + \sigma_B^2 \mathbf{I})^{-1} \mathbf{h}_C^H \\ &= \frac{p_C \|\mathbf{h}_C\|^2}{\sigma_B^2} \left[1 - \frac{\rho^2}{1 + \frac{\sigma_B^2}{p_D \|\mathbf{h}_D\|^2}} \right], \quad (6) \end{aligned}$$

where $\rho = \frac{|\mathbf{h}_C^H \mathbf{h}_D|}{\|\mathbf{h}_C\| \|\mathbf{h}_D\|} \in [-1, 1]$.

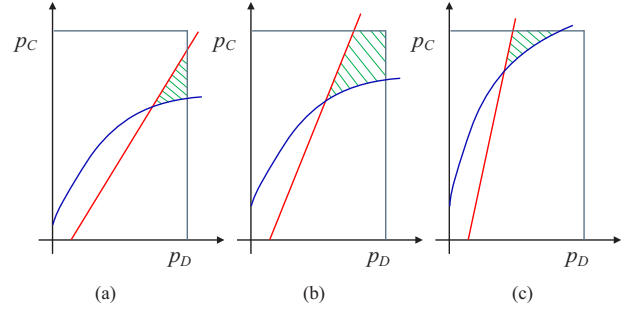


Fig. 2. The feasible region in the p_D - p_C power plane.

B. Power Allocation

Based on the achievable SINR expressions of the CU in (6), we reformulate the constraints (3c)-(3d) as

$$p_C \leq \frac{1}{\alpha k_0} p_D - \frac{\sigma_D^2}{k_0}, \quad (7)$$

$$p_C \geq \beta \left(1 - \frac{k_1 p_D}{p_D + k_2} \right)^{-1}, \quad (8)$$

where $\alpha = \frac{\gamma_D^{\max}}{|h_D|^2}$, $\beta = \frac{\sigma_B^2 \gamma_C^{\max}}{\|\mathbf{h}_C\|^2}$, $k_0 = |h_C|^2$, $k_1 = \rho^2$ and $k_2 = \frac{\sigma_B^2}{\|\mathbf{h}_D\|^2}$. To characterize the feasible region in the p_D - p_C power plane, we take the equation form of constraints (7)-(8) and analyze their first and second derivatives. It can be easily proven that (8) is a concave increasing function. Thus, (7) and (8) can be represented by a red line and a blue curve shown in Fig. 2, respectively. Let \mathcal{P} be the feasible solution region of uplink power, which is characterized by the green shaded area.

Next, defining $\nu_1 = \frac{\|\mathbf{h}_C\|^2}{\sigma_B^2}$ and $\nu_2 = |h_D|^2$, we rewrite the objective in (P1) as $\log R(p_D, p_C)$ where

$$R(p_D, p_C) = \left(1 + \nu_1 p_C \frac{k_2 + \bar{k}_1 p_D}{k_2 + p_D} \right) \left(1 + \frac{\nu_2 p_D}{k_0 p_C + \sigma_D^2} \right). \quad (9)$$

with $\bar{k}_1 = 1 - k_1 \geq 0$.

Proposition 1. The optimal power solution (\hat{p}_D, \hat{p}_C) is at the end of the vertical or horizontal border lines of \mathcal{P} .

Proof: See Appendix A. ■

According to the Proposition 1, we can obtain the closed-form expressions for the optimal power pair in the following three cases. Initially, the intersection points of the red line and the blue curve with the vertical boundary are denoted as $I_L = (p_D^{\max}, I_{Ly})$ and $I_C = (p_D^{\max}, I_{Cy})$, respectively. Then, we have

$$I_{Ly} = \frac{p_D^{\max} - \alpha \sigma_D^2}{\alpha k_0}, \quad I_{Cy} = \frac{\beta (p_D^{\max} + k_2)}{k_1 p_D^{\max} + k_2}. \quad (10)$$

- When $I_{Cy} < I_{Ly} < p_C^{\max}$, as shown in Fig. 2(a), I_L is determined as (\hat{p}_D, \hat{p}_C) .
- When $I_{Cy} < p_C^{\max} < I_{Ly}$, as shown in Fig. 2(b), we have $(\hat{p}_D, \hat{p}_C) = (p_D^{\max}, p_C^{\max})$.
- When $p_C^{\max} < I_{Cy} < I_{Ly}$, as shown in Fig. 2(c), (\hat{p}_D, \hat{p}_C) is chosen from the candidate

pairs $\left\{ \left(\alpha(k_0 p_C^{\max} + \sigma_D^2), p_C^{\max} \right), \left(\frac{k_2(\beta - p_C^{\max})}{k_1 p_C^{\max} - \beta}, p_C^{\max} \right) \right\}$, i.e., the intersection points of the red line and the blue curve with the horizontal boundary.

C. Phase-Shift Design

Given a set of $\{p_C, p_D, \mathbf{w}\}$, we investigate the passive beamforming subproblem. Define $a_{D1} = \sqrt{p_D} g_D$, $\mathbf{b}_{D1}^H = \sqrt{p_D} \mathbf{s}_R^H \text{diag}(\mathbf{s}_T)$, $a_{C1} = \sqrt{p_C} f_C$, $\mathbf{b}_{C1}^H = \sqrt{p_C} \mathbf{s}_R^H \text{diag}(\mathbf{s}_C)$, $a_{C2} = \sqrt{p_C} \mathbf{w}^H \mathbf{g}_C$, $\mathbf{b}_{C2}^H = \sqrt{p_C} \mathbf{w}^H \mathbf{S}_B \text{diag}(\mathbf{s}_C)$, $a_{D2} = \sqrt{p_D} \mathbf{w}^H \mathbf{f}_D$, $\mathbf{b}_{D2}^H = \sqrt{p_D} \mathbf{w}^H \mathbf{S}_B \text{diag}(\mathbf{s}_T)$, and the reflecting coefficients $\boldsymbol{\theta} = [e^{j\theta_1}, e^{j\theta_2}, \dots, e^{j\theta_N}]^T$. Now, (1) and (2) can be rewritten as

$$\begin{aligned} \gamma_D &= \frac{|\sqrt{p_D} g_D + \sqrt{p_D} \mathbf{s}_R^H \boldsymbol{\Theta} \mathbf{s}_T|^2}{|\sqrt{p_C} f_C + \sqrt{p_C} \mathbf{s}_R^H \boldsymbol{\Theta} \mathbf{s}_C|^2 + \sigma_D^2}, \\ &= \frac{|\sqrt{p_D} g_D + \sqrt{p_D} \mathbf{s}_R^H \text{diag}(\mathbf{s}_T) \boldsymbol{\theta}|^2}{|\sqrt{p_C} f_C + \sqrt{p_C} \mathbf{s}_R^H \text{diag}(\mathbf{s}_C) \boldsymbol{\theta}|^2 + \sigma_D^2}, \\ &= \frac{|a_{D1} + \mathbf{b}_{D1}^H \boldsymbol{\theta}|^2}{|a_{C1} + \mathbf{b}_{C1}^H \boldsymbol{\theta}|^2 + \sigma_D^2}, \end{aligned} \quad (11)$$

$$\begin{aligned} \gamma_C &= \frac{|\sqrt{p_C} \mathbf{w}^H \mathbf{g}_C + \sqrt{p_C} \mathbf{w}^H \mathbf{S}_B \boldsymbol{\Theta} \mathbf{s}_C|^2}{|\sqrt{p_D} \mathbf{w}^H \mathbf{f}_D + \sqrt{p_D} \mathbf{w}^H \mathbf{S}_B \boldsymbol{\Theta} \mathbf{s}_T|^2 + \sigma_B^2}, \\ &= \frac{|\sqrt{p_C} \mathbf{w}^H \mathbf{g}_C + \sqrt{p_C} \mathbf{w}^H \mathbf{S}_B \text{diag}(\mathbf{s}_C) \boldsymbol{\theta}|^2}{|\sqrt{p_D} \mathbf{w}^H \mathbf{f}_D + \sqrt{p_D} \mathbf{w}^H \mathbf{S}_B \text{diag}(\mathbf{s}_T) \boldsymbol{\theta}|^2 + \sigma_B^2}, \\ &= \frac{|a_{C2} + \mathbf{b}_{C2}^H \boldsymbol{\theta}|^2}{|a_{D2} + \mathbf{b}_{D2}^H \boldsymbol{\theta}|^2 + \sigma_B^2}, \end{aligned} \quad (12)$$

Using (11) and (12), constraints (3c) and (3d) can be reformulated as

$$|a_{D1} + \mathbf{b}_{D1}^H \boldsymbol{\theta}|^2 - \gamma_D^{\max} (|a_{C1} + \mathbf{b}_{C1}^H \boldsymbol{\theta}|^2 + \sigma_D^2) \geq 0, \quad (13)$$

$$|a_{C2} + \mathbf{b}_{C2}^H \boldsymbol{\theta}|^2 - \gamma_C^{\max} (|a_{D2} + \mathbf{b}_{D2}^H \boldsymbol{\theta}|^2 + \sigma_B^2) \geq 0, \quad (14)$$

Then, problem (P1) is reduced to

$$\begin{aligned} \text{(P3)} : \quad & \max_{\{\boldsymbol{\theta}\}} \log(1 + \gamma_D) + \log(1 + \gamma_C) \\ \text{s.t.} \quad & (13), (14), \\ & |\theta_n| = 1, \quad n = 1, 2, \dots, N, \end{aligned} \quad (15a)$$

Proposition 2. *The original problem (P3) is equivalent to*

$$\begin{aligned} \text{(P4)} : \quad & \max_{\boldsymbol{\theta}} F(\zeta_D, \gamma_D) + F(\zeta_C, \gamma_C) \\ \text{s.t.} \quad & (13), (14), (15a), \end{aligned}$$

where $F(\zeta, \gamma) = \log(1 + \zeta) - \zeta + \frac{(1+\zeta)\gamma}{1+\gamma}$; ζ_D and ζ_C are auxiliary variables. Given $\{\gamma_D, \gamma_C\}$, the optimal ζ_D is equal to γ_D and optimal ζ_C is equal to γ_C .

Proof: See Appendix B. \blacksquare

After applying the transform method proposed in Proposition 2, for a given $\{\zeta_D, \zeta_C\}$, optimizing $\{\gamma_D, \gamma_C\}$ in (P4) can be reformulated as

$$\begin{aligned} \text{(P5)} : \quad & \max_{\boldsymbol{\theta}} \tilde{F}(\gamma_D, \gamma_C) = \frac{\tilde{\zeta}_D \gamma_D}{1 + \gamma_D} + \frac{\tilde{\zeta}_C \gamma_C}{1 + \gamma_C} \\ \text{s.t.} \quad & (13), (14), (15a), \end{aligned}$$

where $\tilde{\zeta}_D = 1 + \zeta_D$ and $\tilde{\zeta}_C = 1 + \zeta_C$. Plugging (11) and (12) into $\tilde{F}(\gamma_D, \gamma_C)$, we have

$$\begin{aligned} \tilde{F}(\boldsymbol{\theta}) &= \frac{\tilde{\zeta}_D |a_{D1} + \mathbf{b}_{D1}^H \boldsymbol{\theta}|^2}{|a_{D1} + \mathbf{b}_{D1}^H \boldsymbol{\theta}|^2 + |a_{C1} + \mathbf{b}_{C1}^H \boldsymbol{\theta}|^2 + \sigma_D^2} \\ &+ \frac{\tilde{\zeta}_C |a_{C2} + \mathbf{b}_{C2}^H \boldsymbol{\theta}|^2}{|a_{C2} + \mathbf{b}_{C2}^H \boldsymbol{\theta}|^2 + |a_{D2} + \mathbf{b}_{D2}^H \boldsymbol{\theta}|^2 + \sigma_B^2}. \end{aligned} \quad (16)$$

Applying the quadratic transform [7] to (16), $\tilde{F}(\boldsymbol{\theta})$ can be reframed as

$$\begin{aligned} \tilde{F}_q(\boldsymbol{\theta}, \xi_D, \xi_C) &= 2\sqrt{\tilde{\zeta}_D} \text{Re} \{ \xi_D^* (a_{D1} + \mathbf{b}_{D1}^H \boldsymbol{\theta}) \} \\ &- |\xi_D|^2 (|a_{D1} + \mathbf{b}_{D1}^H \boldsymbol{\theta}|^2 + |a_{C1} + \mathbf{b}_{C1}^H \boldsymbol{\theta}|^2 + \sigma_D^2) \\ &+ 2\sqrt{\tilde{\zeta}_C} \text{Re} \{ \xi_C^* (a_{C2} + \mathbf{b}_{C2}^H \boldsymbol{\theta}) \} \\ &- |\xi_C|^2 (|a_{C2} + \mathbf{b}_{C2}^H \boldsymbol{\theta}|^2 + |a_{D2} + \mathbf{b}_{D2}^H \boldsymbol{\theta}|^2 + \sigma_B^2), \end{aligned} \quad (17)$$

where ξ_D and ξ_C are complex-valued auxiliary variables. Next, we optimize $\{\xi_D, \xi_C\}$ and $\boldsymbol{\theta}$ alternatively. The optimal $\{\xi_D, \xi_C\}$ for fixed $\boldsymbol{\theta}$ can be computed by setting their first derivatives to zero, as given by

$$\begin{aligned} \hat{\xi}_D &= \frac{\sqrt{\tilde{\zeta}_D} (a_{D1} + \mathbf{b}_{D1}^H \boldsymbol{\theta})}{|a_{D1} + \mathbf{b}_{D1}^H \boldsymbol{\theta}|^2 + |a_{C1} + \mathbf{b}_{C1}^H \boldsymbol{\theta}|^2 + \sigma_D^2}, \\ \hat{\xi}_C &= \frac{\sqrt{\tilde{\zeta}_C} (a_{C2} + \mathbf{b}_{C2}^H \boldsymbol{\theta})}{|a_{C2} + \mathbf{b}_{C2}^H \boldsymbol{\theta}|^2 + |a_{D2} + \mathbf{b}_{D2}^H \boldsymbol{\theta}|^2 + \sigma_B^2}. \end{aligned} \quad (18)$$

The remaining target is to optimize $\boldsymbol{\theta}$ for fixed $\{\xi_D, \xi_C\}$. Expanding the squared terms in (17) yields

$$\begin{aligned} \tilde{F}_q(\boldsymbol{\theta}) &= -\boldsymbol{\theta}^H (\mathbf{B}_1 + \mathbf{B}_2) \boldsymbol{\theta} \\ &+ 2\text{Re} \{ (\mathbf{u}_1 + \mathbf{u}_2)^H \boldsymbol{\theta} \} + (C_1 + C_2), \end{aligned} \quad (19)$$

where

$$\mathbf{B}_1 = |\xi_D|^2 (\mathbf{b}_{D1} \mathbf{b}_{D1}^H + \mathbf{b}_{C1} \mathbf{b}_{C1}^H), \quad (20)$$

$$\mathbf{B}_2 = |\xi_C|^2 (\mathbf{b}_{C2} \mathbf{b}_{C2}^H + \mathbf{b}_{D2} \mathbf{b}_{D2}^H), \quad (21)$$

$$\mathbf{u}_1 = \sqrt{\tilde{\zeta}_D} \xi_D \mathbf{b}_{D1} - |\xi_D|^2 (a_{D1} \mathbf{b}_{D1} + a_{C1} \mathbf{b}_{C1}), \quad (22)$$

$$\mathbf{u}_2 = \sqrt{\tilde{\zeta}_C} \xi_C \mathbf{b}_{C2} - |\xi_C|^2 (a_{C2} \mathbf{b}_{C2} + a_{D2} \mathbf{b}_{D2}), \quad (23)$$

$$C_1 = 2\sqrt{\tilde{\zeta}_D} \text{Re} \{ \xi_D^* a_{D1} \} - |\xi_D|^2 (|a_{D1}|^2 + |a_{C1}|^2 + \sigma_D^2), \quad (24)$$

$$C_2 = 2\sqrt{\tilde{\zeta}_C} \text{Re} \{ \xi_C^* a_{C2} \} - |\xi_C|^2 (|a_{C2}|^2 + |a_{D2}|^2 + \sigma_B^2). \quad (25)$$

After dropping the constant terms in (19) and expanding the squared terms in constraints (13) and (14), (P5) is then reformulated as

$$\begin{aligned} \text{(P6)} : \quad & \max_{\boldsymbol{\theta}} -\boldsymbol{\theta}^H \mathbf{B} \boldsymbol{\theta} + 2\text{Re} \{ \mathbf{u}^H \boldsymbol{\theta} \} \\ \text{s.t.} \quad & \boldsymbol{\theta}^H \mathbf{R}_1 \boldsymbol{\theta} + 2\text{Re} \{ \mathbf{t}_1^H \boldsymbol{\theta} \} + \delta_1 \geq 0, \quad (26a) \\ & \boldsymbol{\theta}^H \mathbf{R}_2 \boldsymbol{\theta} + 2\text{Re} \{ \mathbf{t}_2^H \boldsymbol{\theta} \} + \delta_2 \geq 0, \quad (26b) \end{aligned} \quad (15a),$$

where $\mathbf{B} = \mathbf{B}_1 + \mathbf{B}_2$, $\mathbf{u} = \mathbf{u}_1 + \mathbf{u}_2$, $\mathbf{R}_{D1} = \mathbf{b}_{D1} \mathbf{b}_{D1}^H$, $\mathbf{R}_{C1} = \mathbf{b}_{C1} \mathbf{b}_{C1}^H$, $\mathbf{R}_{D2} = \mathbf{b}_{D2} \mathbf{b}_{D2}^H$, $\mathbf{R}_{C2} = \mathbf{b}_{C2} \mathbf{b}_{C2}^H$,

$\mathbf{R}_1 = \mathbf{R}_{D1} - \gamma_D^{\max} \mathbf{R}_{C1}$, $\mathbf{R}_2 = \mathbf{R}_{C2} - \gamma_C^{\max} \mathbf{R}_{D2}$, $\mathbf{t}_{D1} = a_{D1} \mathbf{b}_{D1}$, $\mathbf{t}_{C1} = a_{C1} \mathbf{b}_{C1}$, $\mathbf{t}_{D2} = a_{D2} \mathbf{b}_{D2}$, $\mathbf{t}_{C2} = a_{C2} \mathbf{b}_{C2}$, $\mathbf{t}_1 = \mathbf{t}_{D1} - \gamma_D^{\max} \mathbf{t}_{C1}$ and $\mathbf{t}_2 = \mathbf{t}_{C2} - \gamma_C^{\max} \mathbf{t}_{D2}$, $\delta_1 = |a_{D1}|^2 - \gamma_D^{\max} (|a_{C1}|^2 + \sigma_D^2)$ and $\delta_2 = |a_{C2}|^2 - \gamma_C^{\max} (|a_{D2}|^2 + \sigma_B^2)$. The problem (P6) is a quadratically constrained quadratic problem (QCQP). Introduce $\bar{\boldsymbol{\theta}} = [\boldsymbol{\theta}^T, 1]^T$, $\Phi = \bar{\boldsymbol{\theta}} \bar{\boldsymbol{\theta}}^H$. Using semi-definite relaxation (SDR) technique, (P6) can be recast as

$$(P7) : \min_{\boldsymbol{\theta}} \text{tr}(\mathbf{R}_B \Phi)$$

$$\text{s.t.} \quad \text{tr}(\bar{\mathbf{R}}_{D1} \Phi) - \gamma_D^{\max} \text{tr}(\bar{\mathbf{R}}_{C1} \Phi) + \delta_1 \geq 0, \quad (27a)$$

$$\text{tr}(\bar{\mathbf{R}}_{C2} \Phi) - \gamma_C^{\max} \text{tr}(\bar{\mathbf{R}}_{D2} \Phi) + \delta_2 \geq 0, \quad (27b)$$

$$\Phi \succeq \mathbf{0}, [\Phi]_{n,n} = 1, n = 1, 2, \dots, N \quad (27c)$$

where

$$\mathbf{R}_B = \begin{bmatrix} \mathbf{B} & -\mathbf{u} \\ -\mathbf{u}^H & 0 \end{bmatrix}, \bar{\mathbf{R}}_{D1} = \begin{bmatrix} \mathbf{R}_{D1} & \mathbf{t}_{D1} \\ \mathbf{t}_{D1}^H & 0 \end{bmatrix},$$

$$\bar{\mathbf{R}}_{C1} = \begin{bmatrix} \mathbf{R}_{C1} & \mathbf{t}_{C1} \\ \mathbf{t}_{C1}^H & 0 \end{bmatrix}, \bar{\mathbf{R}}_{C2} = \begin{bmatrix} \mathbf{R}_{C2} & \mathbf{t}_{C2} \\ \mathbf{t}_{C2}^H & 0 \end{bmatrix},$$

$$\bar{\mathbf{R}}_{D2} = \begin{bmatrix} \mathbf{R}_{D2} & \mathbf{t}_{D2} \\ \mathbf{t}_{D2}^H & 0 \end{bmatrix}. \quad (28)$$

This can be efficiently solved by CVX tools. Then, the Gaussian randomization technique is adopted to obtain a rank-one solution based on the solution obtained from SDR.

IV. SIMULATION RESULTS

Simulation results are provided to evaluate the performance of our proposed algorithm and potential benefits of deploying IRS in D2D systems. We use d_D , d_{DB} , d_{CB} , d_{CD} , d_{SB} , d_{SC} , d_{SR} , d_{ST} and d_0 to denote the the distances between the D2D pairs, DT and BS, CU and BS, CU and DR, RIS and BS, RIS and CU, RIS and DR, RIS and DT and the cell radius, respectively. Assume that the BS, the CU, the DT and the DR are located at $(0, 0)$, $(0, 0.5d_0)$, $(0, -0.75d_0 - 0.5d_D)$ and $(0, -0.75d_0 + 0.5d_D)$, respectively. We set $d_D = 0.2d_0$, $\sigma_B^2 = \sigma_D^2 = 1$, $\gamma_D^{\max} = \gamma_C^{\max} = 3\text{dB}$, $p_D^{\max} = p_C^{\max} = P_m$. Assume that all the channels are zero-mean complex Gaussian with variance $(d/d_0)^{-4}$ where d is the link distance [2]. Additionally, we take $M = 4$.

Fig. 4 compare the achievable sum-rate of different schemes versus the number of reflecting elements. We consider that the RIS is located at $(-0.5d_0, 0.35d_0)$ and $P_m = 10\text{dBW}$. We see that the sum rate of the proposed algorithm with RIS exhibits the superiority over the scheme without RIS. Moreover, the performance gap increases as N grows. This implies that the higher reflection gain can be achieved by passive beamforming of RIS when more RIS elements deployed.

Fig. 5 investigates the impact of normalized maximum power P_m/σ_B^2 on sum-rate achieved by different schemes. Here, the RIS is located at $(-0.5d_0, 0.35d_0)$ and we set $N = 8$. We consider that the RIS is located at $(-0.5d_0, 0.35d_0)$ and $P_m = 10\text{dBW}$. As expected, the sum rate gain of all schemes improve significantly as P_m/σ_B^2 increases. It can be observed that the sum rate of the proposed algorithm

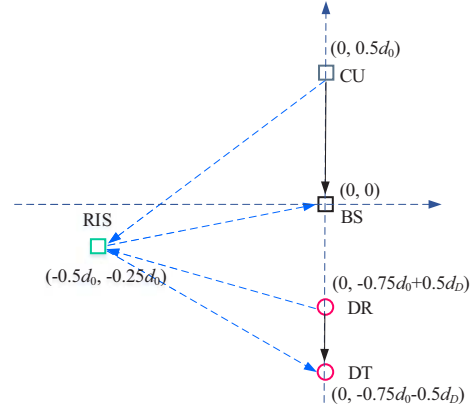


Fig. 3. Simulation setups.

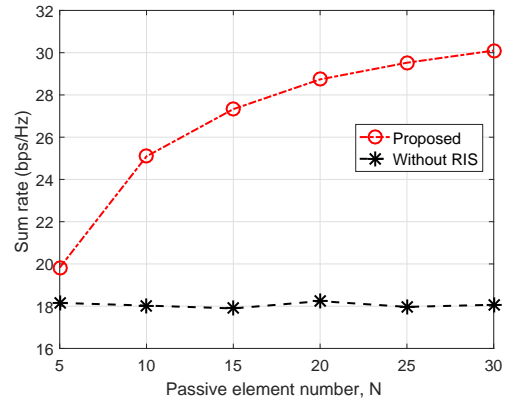


Fig. 4. Achievable sum-rate versus number of reflecting elements.

with RIS outperforms its counterparts without RIS. Thus, we conclude that the RIS has a positive enhancement effect on the achievable rate while meeting the SINR requirements of both CU and D2D pairs.

V. CONCLUSION

This letter proposed a joint design of power control and passive beamforming to maximize the sum-rate in a new IRS-assisted D2D communication system. The IRS assisted scheme with our proposed BCD algorithm was verified by simulation results beneficial to the D2D system performance improvement.

APPENDIX A PROOF OF PROPOSITION 1

Given any point (p_x, p_y) inside the feasible region, there always exists a constant $\varepsilon > 1$ such that $(\varepsilon p_x, \varepsilon p_y) \in \mathcal{P}$. Note that

$$R(p_x, p_y) = \left[1 + \nu_1 p_y \frac{\varepsilon k_2 + \bar{k}_1 \varepsilon p_x}{\varepsilon k_2 + \varepsilon p_x} \right] \left(1 + \frac{\nu_2 \varepsilon p_x}{k_0 \varepsilon p_y + \varepsilon \sigma_D^2} \right),$$

$$< \left[1 + \nu_1 p_y \frac{\varepsilon k_2 + \bar{k}_1 \varepsilon^2 p_x}{k_2 + \varepsilon p_x} \right] \left(1 + \frac{\nu_2 \varepsilon p_x}{k_0 \varepsilon p_y + \sigma_D^2} \right),$$

$$= R(\varepsilon p_x, \varepsilon p_y), \quad (29)$$

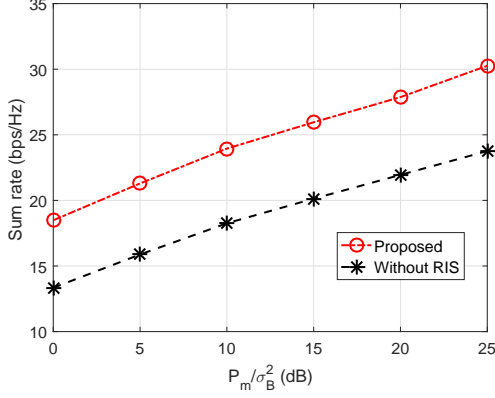


Fig. 5. Achievable sum-rate versus normalized maximum power.

which implies that the optimal power pair is lying on the vertical or horizontal border lines of \mathcal{P} . We denote the vertical or horizontal border lines as $R_C(p_C) = R(p_D^{\max}, p_C)$ and $R_D(p_D) = R(p_D, p_C^{\max})$, respectively. Then, expanding the multiplication expressions of $R_D(p_D)$ yields

$$R_D(p_D) = R_{D1}(p_D) + \nu_1 p_C^{\max} R_{D2}(p_D), \quad (30)$$

where

$$R_{D1}(p_D) = 1 + \nu_1 p_C^{\max} + \frac{\nu_2 p_D}{k_0 p_C^{\max} + \sigma_D^2}, \quad (31)$$

$$R_{D2}(p_D) = \frac{\nu_2 \bar{k}_1 p_D + \nu_2 k_2 - k_1 (k_0 p_C^{\max} + \sigma_D^2)}{(k_0 p_C^{\max} + \sigma_D^2) \left(\frac{k_2}{p_D} + 1 \right)}. \quad (32)$$

It can be seen from (30)-(32) that $R_D(p_D)$ is a strictly increasing function. Then, taking the first derivative of $R_C(p_C)$ yields

$$\frac{dR_C(p_C)}{dp_C} = k_3 \nu_1 + \frac{\nu_2 p_D^{\max} k_4}{(k_0 p_C + \sigma_B^2)^2}, \quad (33)$$

where

$$k_3 = \frac{k_2 + \bar{k}_1 p_D^{\max}}{k_2 + p_D^{\max}}, \quad (34)$$

$$k_4 = \sigma_B^2 k_3 \nu_1 - k_0. \quad (35)$$

We can conclude that when $k_4 \geq 0$ holds, $R_C(p_C)$ is a strictly increasing function. When $k_4 < 0$ holds, $R_C(p_C)$ can be proven to be a convex function by taking its second derivative. This indicates that $R_C(p_C)$ is either an increasing or convex function. The analysis above completes our proof.

APPENDIX B PROOF OF PROPOSITION 2

Note that $F(\zeta, \gamma) = \log(1 + \zeta) - \zeta + \frac{(1+\zeta)\gamma}{1+\gamma}$ is a concave differentiable function with respect to ζ when given γ . Thus, setting $\frac{\partial F}{\partial \zeta}$ to zero yields $\hat{\zeta} = \gamma$. Based on this fundamental result, substituting the obtained solution $\{\hat{\zeta}_D, \hat{\zeta}_C\}$ back in the objective function of (P4) can be recast to the objective function in (P3). As such, the optimal objective values of these two problems are equal and their equivalence is established.

REFERENCES

- [1] Y. Wang, M. Chen, N. Huang, Z. Yang, and Y. Pan, "Joint power and channel allocation for D2D underlying cellular networks with rician fading," *IEEE Commun. Lett.*, vol. 22, no. 12, pp. 2615–2618, Dec. 2018.
- [2] A. Ramezani-Kebrya, M. Dong, B. Liang, G. Boudreau, and S. H. Seyed-mehdi, "Joint power optimization for device-to-device communication in cellular networks with interference control," *IEEE Trans. Wireless Commun.*, vol. 16, no. 8, pp. 5131–5146, Aug. 2017.
- [3] L. Li, T. J. Cui, W. Ji, S. Liu, J. Ding, X. Wan, Y. B. Li, M. Jiang, C.-W. Qiu, and S. Zhang, "Electromagnetic reprogrammable coding-metasurface holograms," *Nature Commun.*, vol. 8, no. 1, p. 197, 2017.
- [4] C. Liaskos, S. Nie, A. Tsioliariidou, A. Pitsillides, S. Ioannidis, and I. Akyildiz, "A new wireless communication paradigm through software-controlled metasurfaces," *IEEE Commun. Mag.*, vol. 56, no. 9, pp. 162–169, Sep. 2018.
- [5] D. Hwang, D. I. Kim, and T. Lee, "Throughput maximization for multiuser MIMO wireless powered communication networks," *IEEE Trans. Veh. Technol.*, vol. 65, no. 7, pp. 5743–5748, Jul. 2016.
- [6] F. Hiai and D. Petz, *Introduction to matrix analysis and applications*. Springer Science & Business Media, 2014.
- [7] K. Shen and W. Yu, "Fractional programming for communication systems: part I: Power control and beamforming," *IEEE Trans. Signal Process.*, vol. 66, no. 10, pp. 2616–2630, May 2018.